Nonreciprocal guided modes in photonic crystals of magnetic garnet particles with a planar defect

Aristi Christofi* and Nikolaos Stefanou

University of Athens, Department of Solid State Physics, Panepistimioupolis, GR-157 84 Athens, Greece
**Corresponding author: aristi@ims.demokritos.gr*

Received May 30, 2014; revised June 26, 2014; accepted July 14, 2014;
posted July 22, 2014 (Doc. ID 213171); published August 13, 2014

It is shown that a planar defect in the stacking sequence of an all-dielectric photonic crystal of garnet spheres strongly supports localized optical guided modes, which originate from Mie resonances of the individual spheres. If the defect breaks space-inversion symmetry and the garnet particles are magnetized inplane, nonreciprocal and lossless transport of light on the defect plane, expected on the basis of group theory in the Voigt–Cotto–Mouton configuration, is demonstrated in ultrathin films of the defect crystal by means of full electrodynamic calculations using the layer-multiple-scattering method properly extended to photonic crystals of gyrotropic spheres. © 2014 Optical Society of America

OCIS codes: (160.3820) Magneto-optical materials; (290.4210) Multiple scattering; (310.2790) Guided waves; (160.5293) Photonic bandgap materials.
http://dx.doi.org/10.1364/JOSAB.31.002104

1. INTRODUCTION

Nonreciprocal photonic structures that lack both space-inversion and time-reversal symmetries [1] have attracted considerable interest in recent years for a variety of reasons. These structures include new physics such as the emergence of topologically protected one-way photonic edge modes [2–5] as well as technologically important devices such as circulators and isolators, all of which are described by a nonsymmetric scattering matrix [6]. Among the different architectures, layered composites provide a versatile platform for realizing asymmetric heterostructures, while breaking of time-reversal symmetry can be accomplished with magneto-optical effects driven by external or internal magnetic fields. Along this line, it has been shown that a planar waveguide formed at a metal/photonic crystal interface supports one-way electromagnetic (EM) modes under the action of a static uniform magnetic field [7], which, however, must be prohibitively strong, of the order of 10^3–10^4 T. In an alternative design with the photonic crystal made from a transparent dielectric material that exhibits strong magneto-optical activity such as bismuth iron garnet, nonreciprocity was found at relatively weak magnetic fields [8]. Moreover, the occurrence of nonreciprocal guided modes has been demonstrated in a periodic monolayer of magnetized plasma particles supported by a dielectric substrate [9] and of magnetic garnet particles on a plasma surface [10]. On the other hand, tunable one-way terahertz plasmonic waveguides based on nonreciprocal magnetoplasmons in metal/dielectric/semiconductor slabs under an external magnetic field have also been proposed [11,12]. It is worth-noting that in all of these layered structures symmetry dictates that nonreciprocal light transport occurs in the transversal Voigt–Cotton–Mouton configuration in which the applied magnetic field is parallel to the interfaces and perpendicular to the wave propagation direction [13].

In the present paper we report a detailed theoretical study of an all-dielectric photonic crystal made of magnetic garnet spheres with a single planar defect, which supports nonreciprocal guided modes. The proposed structure does not suffer from dissipative losses as is the case in magnetoplasmonic architectures due to the strong localization of the wave field at the defect plane/Even a thin film of the crystal consisting of a few layers with the defect operates as an efficient waveguide allowing for the design of ultracompact nonreciprocal devices.

2. METHOD OF CALCULATION

At visible and infrared frequencies, the gyrotropic response of magnetic materials is rather weak and can be described by a relative magnetic permeability $\mu_g = 1$ and a relative electric permittivity tensor of the form

$$\overleftrightarrow{\epsilon_g} = \epsilon \begin{pmatrix} 1 & -ig & 0 \\ ig & 1 & 0 \\ 0 & 0 & 1 \end{pmatrix}, \tag{1}$$

if the magnetization points in the z direction. In the present work we assume $\epsilon = 6.25$ and $g = 0.01$, which are achievable with magnetic garnets [14–16].

Our calculations are based on the full-electrodynamic layer-multiple-scattering method that we recently extended to photonic structures of gyrotropic spheres. A detailed description of the method can be found elsewhere [17–19]. Here we restrict ourselves in noting that we evaluate the scattering T matrix of the single gyrotropic sphere in a spherical-wave basis from a set of coupled linear equations that relate the expansion coefficients of the scattered to those of the incident field [19–23]. If the gyration vector is oriented along the z direction, the T matrix has a block diagonal form:

$$T_{Plm;P'l'm'} = T^{(m)}_{Pl;P'l'}\delta_{mm'},$$

where P stands for the polarization mode, magnetic (H) or electric (E), and l, m are the usual angular momentum indices. Moreover, $T^{(m)}_{Pl;P'l'}$ vanishes identically if the magnetic/electric multipoles corresponding to Pl and $P'l'$ do not have the same parity, even or odd, which means that the T matrix in a given m subspace is further reduced into two submatrices. The above symmetry properties, however, do not hold in any coordinate system. In general, if α, β, γ are the Euler angles transforming an arbitrarily chosen coordinate system into the given coordinate system in which the gyration vector is oriented along the z axis, the T matrix is given by [24]

$$T_{Plm;P'l'm'} = \sum_{m''} D^{(l)}_{mm''}(\alpha,\beta,\gamma)T^{(m'')}_{Pl;P'l'}D^{(l')}_{m''m'}(-\gamma,-\beta,-\alpha), \quad (2)$$

where $D^{(l)}$ are the appropriate transformation matrices associated with the l irreducible representation of the $O(3)$ group [25].

3. RESULTS AND DISCUSSION

The optical response of a single unmagnetized garnet sphere [$g = 0$ in Eq. (1)] of radius S is characterized by strong and spectrally separated magnetic (H) and electric (E) multipole (2^l-pole, $l = 1, 2, 3, \ldots$) Mie resonances with increased field intensity in the region of the sphere [26]. If such spheres are assembled into a sparse periodic structure, narrow photonic bands of collective Bloch states are formed from the resonant modes of the individual particles, weakly interacting between them. The wavefield associated with these states maintains a strongly localized character in the region of the spheres. In addition to the above narrow bands, there are of course extended bands of propagating modes in the homogeneous host medium, which are folded within the first Brillouin zone because of the periodic structure, while Bragg gaps open up at the Brillouin zone boundaries. Anticrossing interaction between narrow and extended bands of the same symmetry gives rise to the formation of additional frequency gaps and hybridized bands that have strong admixture of the localized modes in their flat parts, near the boundaries and the center of the first Brillouin zone.

Such a photonic band diagram, along the [001] direction of a simple cubic crystal of unmagnetized garnet spheres with radius to lattice constant ratio $S/a = 0.3$ in air, is shown in Fig. 1(a). Along the given crystallographic direction, the bands have the symmetry of the irreducible representations of the C_{4v} point group [25], and thus they are either nondegenerate or doubly degenerate. It is worth noting that only the doubly degenerate bands can be excited by light incident normally on a finite (001) slab of the crystal. The nondegenerate bands are optically inactive because they do not have the proper symmetry in a finite (001) slab of the crystal corresponding to bound states of the EM field that decrease exponentially outside the slab on either side of it. Apart from the ordinary frequency bands, which correspond to real values of the z component of the wave vector k_z, in Fig. 1(a) we show the gap regions with dotted lines, the optically active doubly degenerate real-frequency lines with the smallest in magnitude imaginary part of k_z, which determine the attenuation of the wave field over these regions. The extinction of light

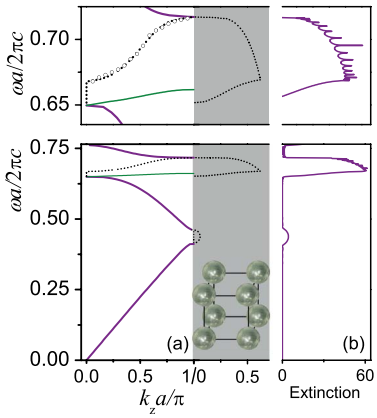

Fig. 1. (a) Photonic band structure of a simple cubic crystal of unmagnetized garnet spheres, with radius to lattice constant ratio $S/a = 0.3$, in air, (see inset) along its [001] direction. Thick and thin lines denote doubly degenerate and nondegenerate bands, respectively. Over the frequency gaps with dotted lines we display the doubly degenerate real frequency lines with the smallest in magnitude imaginary part, which is depicted in the shaded region. (b) Corresponding extinction spectrum for light incident normally on a slab consisting of 16 (001) planes of spheres of the given crystal. In the upper part of the figure we show an enlarged view of the diagrams in the frequency region about the second band gap.

propagating through the crystal, if its angular frequency ω lies within a band gap, is $2d\,\mathrm{Im}[k_z(\omega)] + \text{const.}$, where d is the propagation distance for a given value of the x–y component of the wave vector [see Fig. 1(b)].

It can be seen from Fig. 1 that there are two gaps in the frequency region under consideration. The lowest frequency gap is a Bragg gap, while the second gap is a hybridization-induced gap, which arises from anticrossing interaction between the extended effective-medium band and a narrow band that originates from the fundamental magnetic dipole resonant modes of the individual spheres [26]. A more detailed analysis of the formation of this hybridization gap can be found elsewhere [27]. The attenuation within the first (Bragg) gap is relatively small, but within the second (hybridization) gap it is very strong, which is the case for other directions in reciprocal space as well. A big advantage of using this hybridization gap instead of a structural Bragg gap in unidirectional configurations in order to suppress radiative modes [7] is precisely the very strong attenuation that can be achieved even with a thin film of the crystal consisting of a few layers of spheres. There is also an interesting observation to be made about the section of the real-frequency line over the hybridization gap with k_z complex and $0 \le \mathrm{Re}[k_z] \le \pi/a$. The band structure of Fig. 1(a) applies to the infinite crystal, and the corresponding extinction spectrum in Fig. 1(b) reflects the properties of a slab of 16 planes of spheres. The resonances in the extinction of the slab, which is defined as minus the natural logarithm of the transmittance, suggest that at the corresponding frequencies there exist resonances of some kind in the slab, and we observe that these resonances appear within the frequency gap of the infinite crystal. These resonances (of the slab) are clearly due to resonances of the wave field localized on the individual spheres interacting very weakly between them. Of course, there cannot be states of the EM field in the infinite crystal within the gap, i.e., with complex k_z. But in a slab of finite thickness, such evanescent waves

may exist and may lead to resonances of the EM field with a high amplitude at the surface of the slab (within the spheres of the surface planes) and a much smaller amplitude in the middle of the slab (within the spheres of the middle planes). It is worth noting that the resonances of the slab appear at the frequencies along the real-frequency line corresponding to $\mathrm{Re}[k_z]a/\pi = \kappa/(N_L+1)$, $\kappa = 1, 2, \ldots, N_L$, where $N_L = 16$ is the number of planes in the given slab as shown by the open circles in the enlarged view of Fig. 1(a). This implies that the number of resonance peaks over the gap region increases with the thickness N_L of the slab.

Within the layer-multiple-scattering formalism, it is straightforward to introduce into the structure a planar defect with the same two-dimensional periodicity by, e.g., replacing the spheres of one particular plane with spheres of different types and/or size, shifting the plane, etc. Here we choose to create a planar defect in the given crystal by shifting a particular (001) lattice plane along the [001] direction so as to break space-inversion symmetry, while time-reversal symmetry is removed by magnetizing the garnet spheres. It has been shown that a planar defect in a photonic crystal gives rise to bands of interface states of the EM field corresponding to frequencies within the frequency gaps of the crystal, which manifest themselves as resonance structures in the transmission spectrum of light incident at a given angle on a finite slab of the material [28]. We consider a slab consisting of just five (001) layers of spheres of the crystal under study, with the middle layer being shifted by 25% along the [001] direction, as shown in Fig. 2(a), and focus on the hybridization gap where the attenuation is very strong, and thus we obtain well localized interface modes that correspond to sharp resonances. If the garnet spheres are magnetized normal to the defect plane, the structure remains invariant under the operations of the C_4 point-symmetry group and spectral reciprocity of the interface modes $\omega(-k_x, -k_y) = \omega(k_x, k_y)$ is always ensured by a rotation through an angle π about the z axis, which is a symmetry operation of C_4 [25]. However, if the garnet spheres are magnetized parallel to the defect plane, say along the y direction, the relevant point symmetry group C_{1h} consists of two operations: identity and reflection with respect to the x–z plane [25]. Therefore, in this case, while reciprocity of the interface modes guided along the magnetization direction, $\omega(0, -k_y) = \omega(0, k_y)$, is ensured by mirror symmetry with respect to the x–z plane, $\omega(-k_x, 0) \neq \omega(k_x, 0)$ because there is no group symmetry operation that transforms $(k_x, 0, 0)$ into $(-k_x, 0, 0)$, given also the lack of time-reversal symmetry. Consequently, since nonreciprocity of interface guided modes is anticipated in the Voigt–Cotton–Mouton geometry with the garnet spheres magnetized inplane, we study this configuration through detailed transmission calculations by systematically varying the angle of incidence in the x–z plane from $-\pi/2$ to $\pi/2$ or, equivalently, by varying k_x and keeping $k_y = 0$. Because of the C_{1h} symmetry of this configuration, the interface modes are either even or odd upon reflection with respect to the x–z plane and can be excited by appropriately incident light polarized in the plane of incidence (p polarization) or normal to the plane of incidence (s polarization), respectively. In this case it is worth noting that since the magnetization is not oriented along the z direction, which is by definition the direction of growth of the crystal in the layer-multiple-scattering method, but along the y direction,

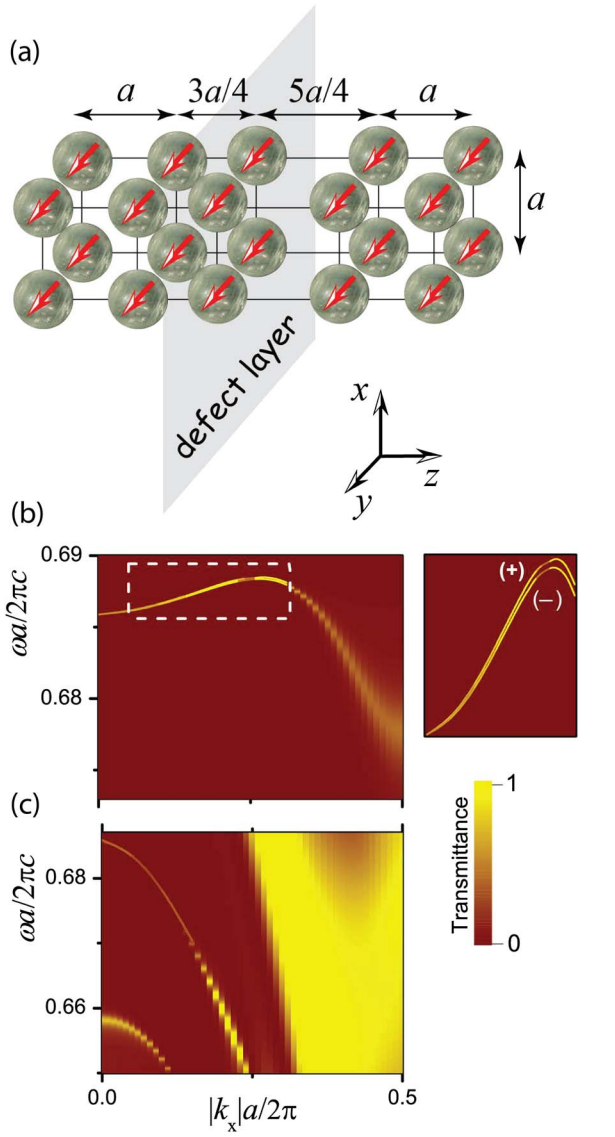

Fig. 2. (a) Five-layers-thick (001) slab of a simple cubic crystal of garnet spheres, in air, with the middle plane displaced by 25% along the [001] direction. The spheres are magnetized along the y direction and their radius is 30% of the lattice constant. Transmittance of the above slab within the hybridization gap of the crystal (see Fig. 1), for s- and p- polarized light [(b) and (c), respectively] incident in the x–z plane at an angle θ corresponding to $k_x = (\omega/c)\sin\theta$. The inset displays an enlarged view (b) in the region indicated by the dashed rectangle, with the (+) and (−) signs denoting positive and negative values of k_x, respectively.

we need to transform the T matrix of the single magnetic garnet sphere according to Eq. (2) using the appropriate Euler angles: $\alpha = 90°$, $\beta = 90°$, and $\gamma = 0°$.

Figure 2 displays the transmission spectra of the slab with the planar defect under consideration within the hybridization gap of the crystal, for s- and p- polarized light incident in the x–z plane, versus the x-component of the wave vector k_x, which defines the angle of incidence $\theta = \arcsin(ck_x/\omega)$. For both polarizations the strongly localized defect guided modes are manifested as sharp transmission peaks for relatively small angles of incidence. As the angle of incidence gets larger the associated frequency gap shrinks and the transmission peaks become broader due to the increasing leakage of the

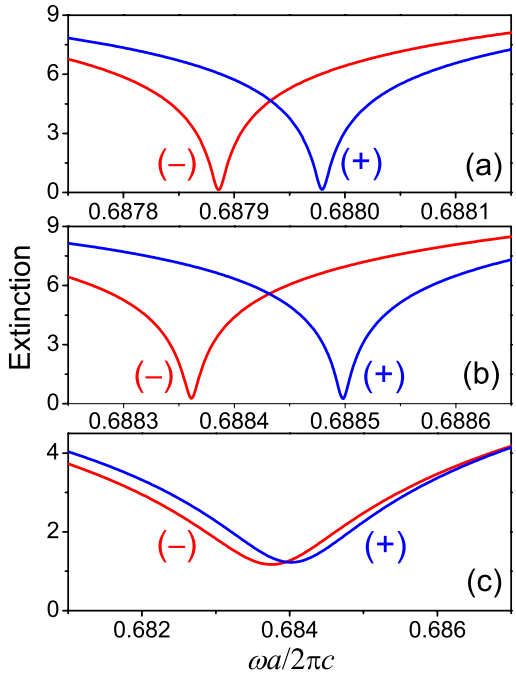

Fig. 3. Extinction spectra of the slab of Fig. 2 for s-polarized light incident in the x–z plane at an angle θ corresponding to (a) $|k_x|a/2\pi = 0.20$, (b) 0.27, and (c) 0.40 [$\theta = \arcsin(k_x c/\omega)$], in the frequency region of the nonreciprocal guided modes. The (+) and (−) signs denote positive and negative values of k_x, respectively.

corresponding modes, which finally merge into the continuum of the photonic bands of the crystal. As can be seen from the enlarged view of Fig. 2(b), there is a spectral splitting of the dispersion curves associated with the forward and backward propagating guided waves in the direction normal to the magnetic field, $\omega(-k_x, 0) \neq \omega(k_x, 0)$, which is a clear signature of nonreciprocity. This can be clearly observed in Fig. 3, where extinction spectra for selected values of $|k_x|a/2\pi = 0.20$, 0.27, and 0.40 corresponding to angles of incidence $\theta = 17°$, 23°, and 30°, respectively, of s-polarized light are displayed. The extinction ratio between forward- and backward-propagation waves reaches values as large as 30–40. However, by increasing the angle of incidence, this ratio decreases because of the broadening of the resonances and becomes vanishingly small.

4. CONCLUSIONS

In summary, by means of rigorous full electrodynamic calculations using the layer multiple-scattering method, we studied the optical response of a three-dimensional crystal of magnetic garnet spheres with a planar defect in the stacking sequence, which breaks space-inversion symmetry. We demonstrated the occurrence of nonreciprocal guided modes, strongly localized on the defect plane even in thin films of the structure (a few layers thick), in the Voigt–Cotton–Mouton configuration for inplane magnetization and provided a consistent interpretation of the underlying physics.

ACKNOWLEDGMENTS

Aristi Christofi is supported by a SPIE Optics and Photonics Education Scholarship.

REFERENCES

1. A. Figotin and I. Vitebsky, "Nonreciprocal magnetic photonic crystals," Phys. Rev. E **63**, 066609 (2001).
2. F. D. M. Haldane and S. Raghu, "Possible realization of directional optical waveguides in photonic crystals with broken time-reversal symmetry," Phys. Rev. Lett. **100**, 013904 (2008).
3. S. Raghu and F. D. M. Haldane, "Analogs of quantum-Hall-effect edge states in photonic crystals," Phys. Rev. A **78**, 033834 (2008).
4. Z. Wang, Y. D. Chong, J. D. Joannopoulos, and M. Soljačić, "Reflection-free one-way edge modes in a gyromagnetic photonic crystal," Phys. Rev. Lett. **100**, 013905 (2008).
5. Z. Wang, Y. D. Chong, J. D. Joannopoulos, and M. Soljačić, "Observation of unidirectional backscattering-immune topological electromagnetic states," Nature **461**, 772–775 (2009).
6. S. Fan, R. Baets, A. Petrov, Z. Yu, J. D. Joannopoulos, W. Freude, A. Melloni, M. Popović, M. Vanwolleghem, D. Jalas, M. Eich, M. Krause, H. Renner, E. Brinkmeyer, and C. R. Doerr, "Comment on nonreciprocal light propagation in a silicon photonic circuit," Science **335**, 38 (2012).
7. Z. Yu, G. Veronis, Z. Wang, and S. Fan, "One-way electromagnetic waveguide formed at the interface between a plasmonic metal under a static magnetic field and a photonic crystal," Phys. Rev. Lett. **100**, 023902 (2008).
8. V. Kuzmiak, S. Eyderman, and M. Vanwolleghem, "Controlling surface plasmon polaritons by a static and/or time-dependent external magnetic field," Phys. Rev. B **86**, 045403 (2012).
9. A. Christofi and N. Stefanou, "Nonreciprocal photonic surface states in periodic structures of magnetized plasma nanospheres," Phys. Rev. B **88**, 125133 (2013).
10. A. Christofi, C. Tserkezis, and N. Stefanou, "Multiple scattering calculations for nonreciprocal planar magnetoplasmonic nanostructures," J. Quant. Spectrosc. Radiat. Transfer **146**, 34–40 (2014).
11. B. Hu, Q. J. Wang, and Y. Zhang, "Broadly tunable one-way terahertz plasmonic waveguide based on nonreciprocal surface magneto plasmons," Opt. Lett. **37**, 1895–1897 (2012).
12. P. Kwiecien, V. Kuzmiak, I. Richter, and J. Ctyroky, "Properties of one-way magnetooptic nanostructures in THz range," in *Proceedings of Progress in Electromagnetics Research Symposium (PIERS)*, Stockholm, Sweden, 2013, pp. 730–735.
13. L. Remer, E. Mohler, W. Grill, and B. Lüthi, "Nonreciprocity in the optical reflection of magnetoplasmas," Phys. Rev. B **30**, 3277 (1984).
14. S. M. Drezdzon and T. Yoshie, "On-chip waveguide isolator based on bismuth iron garnet operating via nonreciprocal single-mode cutoff," Opt. Express **17**, 9276–9281 (2009).
15. A. B. Khanikaev, S. H. Mousavi, G. Shvets, and Y. S. Kivshar, "One-way extraordinary optical transmission and nonreciprocal spoof plasmons," Phys. Rev. Lett. **105**, 126804 (2010).
16. K. Fang, Z. Yu, V. Liu, and S. Fan, "Ultracompact nonreciprocal optical isolator based on guided resonance in a magneto-optical photonic crystal slab," Opt. Lett. **36**, 4254–4256 (2011).
17. N. Stefanou, V. Yannopapas, and A. Modinos, "Heterostructures of photonic crystals: frequency bands and transmission coefficients," Comput. Phys. Commun. **113**, 49–77 (1998).
18. N. Stefanou, V. Yannopapas, and A. Modinos, "MULTEM2: a new version of the program for transmission and band-structure calculations of photonic crystals," Comput. Phys. Commun. **132**, 189–196 (2000).
19. A. Christofi and N. Stefanou, "Layer multiple scattering calculations for nonreciprocal photonic structures," Int. J. Mod. Phys. B **28**, 1441012 (2014).
20. G. W. Ford and S. A. Werner, "Scattering and absorption of electromagnetic waves by a gyrotropic sphere," Phys. Rev. B **18**, 6752 (1978).
21. Z. Lin and S. T. Chui, "Electromagnetic scattering by optically anisotropic magnetic particle," Phys. Rev. E **69**, 056614 (2004).
22. J. L. W. Li and W. L. Ong, "A new solution for characterizing electromagnetic scattering by a gyroelectric sphere," IEEE Trans. Antennas Propag. **59**, 3370–3378 (2011).
23. J. L. W. Li, W. L. Ong, and K. H. R. Zheng, "Anisotropic scattering effects of a gyrotropic sphere characterized using the T-matrix method," Phys. Rev. E **85**, 036601 (2012).

24. M. I. Mishchenko, L. D. Travis, and A. A. Lacis, *Scattering, Absorption, and Emission of Light by Small Particles* (Cambridge, 2002).
25. T. Inui, Y. Tanabe, and Y. Onodera, *Group Theory and its Applications in Physics* (Springer, 1990).
26. A. García-Etxarri, R. Gómez-Medina, L. S. Froufe-Pérez, C. López, L. Chantada, F. Scheffold, J. Aizpurua, M. Nieto-Vesperinas, and J. J. Sáenz, "Strong magnetic response of submicron silicon particles in the infrared," Opt. Express **19**, 4815 (2011).
27. A. Christofi, N. Stefanou, and N. Papanikolaou, "Periodic structures of magnetic garnet particles for strong Faraday rotation enhancement," Phys. Rev. B **89**, 214410 (2014).
28. V. Karathanos, A. Modinos, and N. Stefanou, "Planar defects in photonic crystals," J. Phys. Condens. Matter **6**, 6257–6264 (1994).